# INTEGRATED DESIGN OF TRAJECTORY OPTIMIZATION AND TRACKING GUIDANCE FOR MARS ATMOSPHERIC ENTRY

**Xiuqiang Jiang**[(1)], **Shuang Li**[(2)], **and Junhua Feng**[(3)]
[(1)(2)] *College of Astronautics, Nanjing University of Aeronautics and Astronautics, Nanjing 210016, China, 86-25-84896039, lishuang@nuaa.edu.cn*
[(3)] *Xi'an satellite control center, Xi'an 710043, China, 86-18710362919, 2399442966@qq.com*

***Abstract:*** *In order to improve the accuracy and robustness of reference tracking guidance for Mars atmospheric entry, we developed the integrated design of reference trajectory and optimal guidance method in this paper, which takes into account both the tracking capacity of control system and the effect of uncertainties during Mars atmospheric entry. Firstly, the sensitivity matrixes of system state variables with respect to uncertainties and perturbations along the entry trajectory are defined. The introduction of the sensitivity matrixes is the key to integrated design of reference trajectory optimization and tracking guidance. Secondly, the gain matrix of tracking guidance is contained into the reference trajectory optimization process through the dynamic equations with state sensitivity. The trajectory optimization process and the subsequent tracking guidance process are linked together by the introducing the gain matrix. Thirdly, the performance index of state sensitivity is defined according to specific design requirements (e.g. terminal height, velocity and heading error can be combined and weighted to construct the performance index of state sensitivity), and this performance index is a function of the state sensitivity. Then, the comprehensive performance index can be constructed by using the weight factor method to combine the performance index of state sensitivity and original optimal performance index. Finally, this weighted optimization problem can be easily solved by Gauss Pseudospectral Method (GPM) or other direct optimization algorithms.*

***Keywords:*** *Mars entry, trajectory optimization, tracking guidance, integrated design*

## 1. Introduction

To date, all Mars landers successfully reached the surface of Mars have relied on unguided entry technologies developed for the Viking missions in the mid-seventies of the last century, except for Mars Science Laboratory (MSL), their landing accuracy heavily depend on navigation accuracy of initial entry state. Viking-1/2 landers have a large landing error as $280\times100$ km, and that of Mars Pathfinder (MPF) reached $200\times100$ km. Due to a higher accuracy of initial entry state is required, landing error of Mars Exploration Rover (MER) is reduced to $80\times12$ km, and that of Phoenix reached $100\times21$ km [1]. In addition, uncertainties in Mars atmosphere density and aerodynamic parameters are also one of the most significant error sources leading to large landing dispersion [1,2]. To this end, active guided entry mode is utilized to the MSL in 2012, and its landing error is unprecedentedly reduced to $20\times10$ km. Next-generation Mars landing missions, such as simple return, manned landing and Mars base, require pin-point landing capacity (i.e. the lander need to be landed within 1km from a designed landing point), traditional Mars entry mode and Apollo-like entry guidance is quite incompetent to do this work, advanced Mars entry guidance technologies need to be developed [1-3].

Mars entry guidance task is to deliver an entry vehicle from its initial state to a designated parachute deployment target safely and accurately at the end of the entry phase [1-3]. However, the actual initial entry state errors and uncertainties heavily reduced the performance of guidance [1,2]. NASA's research show that high-precision robust atmospheric entry active close-loop guidance is one of the most essential ways to suppress the adverse effect of initial state errors and uncertainties in the course of Mars entry, and realize pin-point landing on the surface of Mars [4,5]. Hence, it is believed that next-generation Mars pin-point landing missions will basically inherit the ballistic-lifting configuration and guided entry mode utilized in MSL mission [6].

As two integral part of reference tracking guidance, reference trajectory optimization and tracking guidance design are almost carried out separately so far. However, due to the thin atmosphere of Mars, for Mars Science Laboratory-like low lift entry vehicle, the produced aerodynamic force that support effective control operation is relatively small, which severely restrict the tracking capacity of control system [7]. Additionally, there are larger state errors and parameter uncertainties in the course of Mars atmospheric entry, which will lead to the degradation of reference tracking guidance [1,2]. To improve the accuracy and robustness of reference tracking guidance for Mars atmospheric entry, in this paper, we address reference trajectory and optimal guidance integrated design method, which takes both the tracking capacity of control system and the uncertainties during Mars atmospheric entry into account. The weighted optimization problem can be solved by a direct method.

## 2. Problem formulation

### 2.1 Mars entry dynamics

As entry process only lasts a very short time, the MSL-like entry vehicle can be modeled as an unpowered point mass flying in a stationary atmosphere of a non-rotating planet. Entry vehicle is commanded to fly at a constant trim angle of attack, and the controlled guidance of the vehicle is achieved only through modulating the bank angle with a reaction control system (RCS). The three degree-of-freedom (DOF) dynamic equations of Mars entry vehicle, defined with respect to the Mars centered Mars-fixed coordinate system are given by [8,9]

$$\dot{r} = v\sin\gamma \tag{1}$$

$$\dot{v} = -D - g_m \sin\gamma \tag{2}$$

$$\dot{\gamma} = \left(\frac{v}{r} - \frac{g_m}{v}\right)\cos\gamma + \frac{L}{v}\cos\sigma \tag{3}$$

$$\dot{\theta} = \frac{v\cos\gamma\sin\psi}{r\cos\lambda} \tag{4}$$

$$\dot{\lambda} = \frac{v}{r}\cos\gamma\cos\psi \tag{5}$$

$$\dot{\psi} = \frac{v}{r}\sin\psi\cos\gamma\tan\lambda + \frac{L\sin\sigma}{v\cos\gamma} \tag{6}$$

where, $r$ is the distance from the center of Mars to the center of mass of the entry vehicle, $v$ is the velocity of the entry vehicle, $\theta$ is the longitude and $\lambda$ is the latitude, $\gamma$ is the flight path angle. The heading (azimuth) angle is $\psi$, defined as a clockwise rotation angle starting at due north, and $\sigma$ is the bank angle defined as the angle about the velocity vector from the local vertical plane to the lift vector. Mars is treated as a uniform spheroid, and a uniform gravitational field is adopted here, an inverse square gravitational acceleration $g_M = m/r^2$, where $m = GM_{\text{Mars}}$. $L$ and $D$ are the

aerodynamic lift and drag accelerations, defined by $D=\frac{1}{2}\rho v^2 C_D S/m$ and $L=\frac{1}{2}\rho v^2 C_L S/m$, where $C_L$ and $C_D$ are the aerodynamic lift and drag coefficients respectively, $S$ represents the vehicle reference surface area, and $m$ is the mass of the entry vehicle. $\frac{1}{2}\rho v^2$ is termed as dynamic pressure and $C_D S/m$ is named ballistic coefficient, and the Mars atmospheric density $\rho$ is defined as $\rho = \rho_0 \exp[-(r-r_0)/h_s]$, where $\rho_0$ is the density on the surface of Mars, $r_0$ is the radius of the Mars, $h_s$ is the constant scale height. Due to the angle of attack is assumed to follow the aerodynamic trim angle and the Mars entry dynamic equations are only related with the bank angle $\sigma$, so the attitude motion equations can be simplified to one DOF and only roll channel need to be considered. It yields $\dot{\sigma} = w$ and $\dot{w} = a$, where $\omega$ and $\alpha$ are the bank angular rate and acceleration, respectively.

From equations (1)~(6), it can be easily found that the longitudinal and downrange motion equations are decoupled with lateral/heading motion equations. Hence, for Mars entry guidance law, bank angle modulation only need be designed by taking the longitudinal motion profile into account first. Then, the bank reversal maneuver logic is adopted to ensure the entry vehicle to follow the symmetric lateral error corridor and reach the target position. Thus, longitude and latitude integrations are not required in this reduced dynamics formulation since they are replaced by the downrange. The longitudinal dynamic equations are given as follows [8,9]

$$\dot{r} = v\sin\gamma \tag{7}$$

$$\dot{v} = -D - g_m \sin\gamma + d_3 \tag{8}$$

$$\dot{\gamma} = \left(\frac{v}{r} - \frac{g_m}{v}\right)\cos\gamma + \frac{L}{v}u + d_4 \tag{9}$$

$$\dot{s} = v\cos\gamma \tag{10}$$

where $d_3$ and $d_4$ are the uncertain disturbance terms from Martian atmospheric density and aerodynamic parameters. In addition, the longitudinal/downrange dynamics are given by equation (10), and the lateral dynamics are defined through the azimuth equation in equation (6).

### 2.2 Performance Function

The performance function consists of terminal height, fuel consumption, and tracking control performance. It is expressed as follows.

$$J = -h(t_f) + c_s J_S + c_u J_u \tag{11}$$

where, $c_s$ and $c_u$ are weight coefficient, $J_u = \int_{t_0}^{t_f} \dot{\sigma}^2 dt$ denotes the fuel consumption index , $J_S$ denotes the sensitivity index which reflects the level of uncertainty influence the trajectory.

### 2.3 Constraints

(1) Initial constraints, including initial flight height, velocity, flight path angle, and range.

$$r(t_0) = r_0\ ,\ v(t_0) = v_0\ ,\ g\ (t_0) = g_0\ ,\ s(t_0) = s_0 \tag{12}$$

(2) Terminal constraints.

In order to meet the requirements of predesigned area and velocity at the parachute deployment point, the terminal constraints are expressed as follows.

$$s(t_f) = s_f\ , v(t_f) < v_f\ , \text{terminal time } t_f \text{ is free} \tag{13}$$

(3) Path constraints.

The entry vehicle's normal overload, dynamic pressure and aerodynamic heating rate should meet certain constraints during Mars atmospheric entry process [8]

$$n_a = \sqrt{L^2 + D^2} \le n_{\max} \tag{14}$$

$$q = \tfrac{1}{2} r v^2 \le q_{\max} \tag{15}$$

$$\dot{Q} = a r^{0.5} v^k \le \dot{Q}_{\max} \tag{16}$$

where, $n_a, q, \dot{Q}$ are the normal overload, dynamic pressure and aerodynamic heating rate, respectively, $n_{\max}, q_{\max}, \dot{Q}_{\max}$ are the tolerable maximum values, $a$ and $k$ are the heat flux-related coefficients.

(4) Control constraints

Mars entry vehicle only has limited maneuverability, which usually leads to strict terminal constraints. In order to satisfy the requirements of control system, the control input $u$ and the maneuver rate of bank angle $\dot{s}$ are constrained with prescribed bounds as follows [8]

$$s_{\min} \le s \le s_{\max} \tag{17}$$

$$\dot{s}_{\min} \le \dot{s} \le \dot{s}_{\max} \tag{18}$$

$$\ddot{s}_{\min} \le \ddot{s} \le \ddot{s}_{\max} \tag{19}$$

where, $u$ is defined as $u = \cos s$ .

## 3. Integrated design of optimal trajectory and tracking guidance

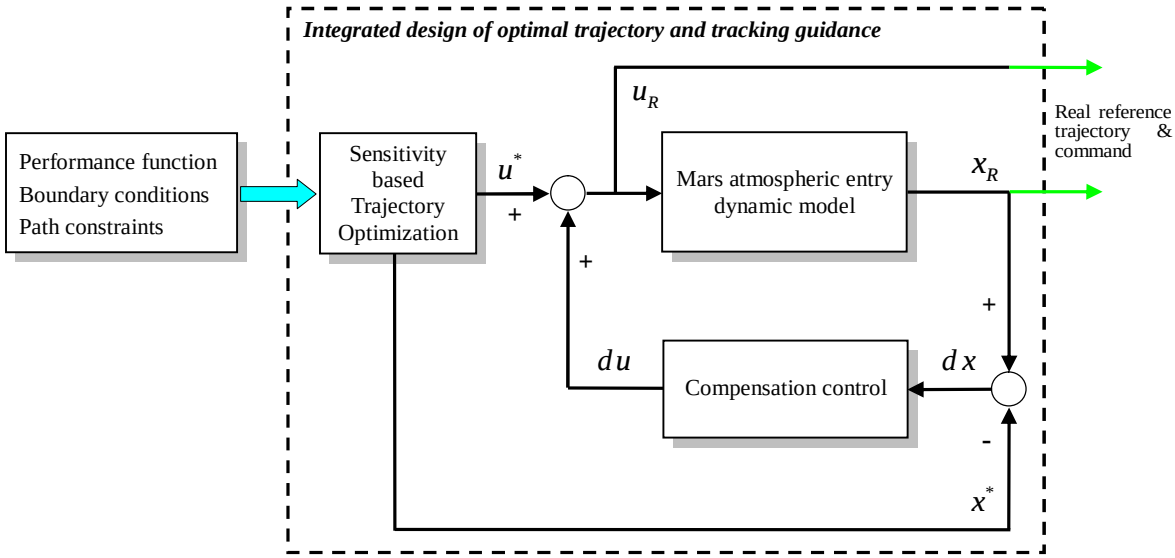


**Figure 1. Sketch of integrated design of optimal trajectory and tracking guidance**

### 3.1 Main idea

As shown in figure 1, the main idea of integrated design of optimal trajectory and tracking guidance including: defined and input the performance function, boundary conditions, and path constraints; sensitivity based trajectory optimization module considered dynamical uncertainty and control authority, it outputs a basic reference trajectory and command; optimal compensation

control module considered control system configuration, it outputs a compensation command based on the trajectory error with respect to the basic reference trajectory; the outputs of the entire integrated design ($x_R$ and $u_R$) are treated as the real reference trajectory and real reference command, and provide to the subsequent tracking guidance system.

### 3.2 Reference Trajectory Generating

Due to the thin atmosphere of Mars and low lifting body configuration, Mars entry vehicles have only low control authority, which severely limit the performance of tracking guidance and control system. At the same time, there are larger state errors and parameter uncertainties in the course of Mars atmospheric entry, which will lead to the degradation of reference tracking guidance algorithms. Hence, reference trajectory generating should consider both the tracking control capacity and the effect of uncertainties during Mars atmospheric entry. This kind of reference trajectory generating is described as figure 2 using mathematical language.

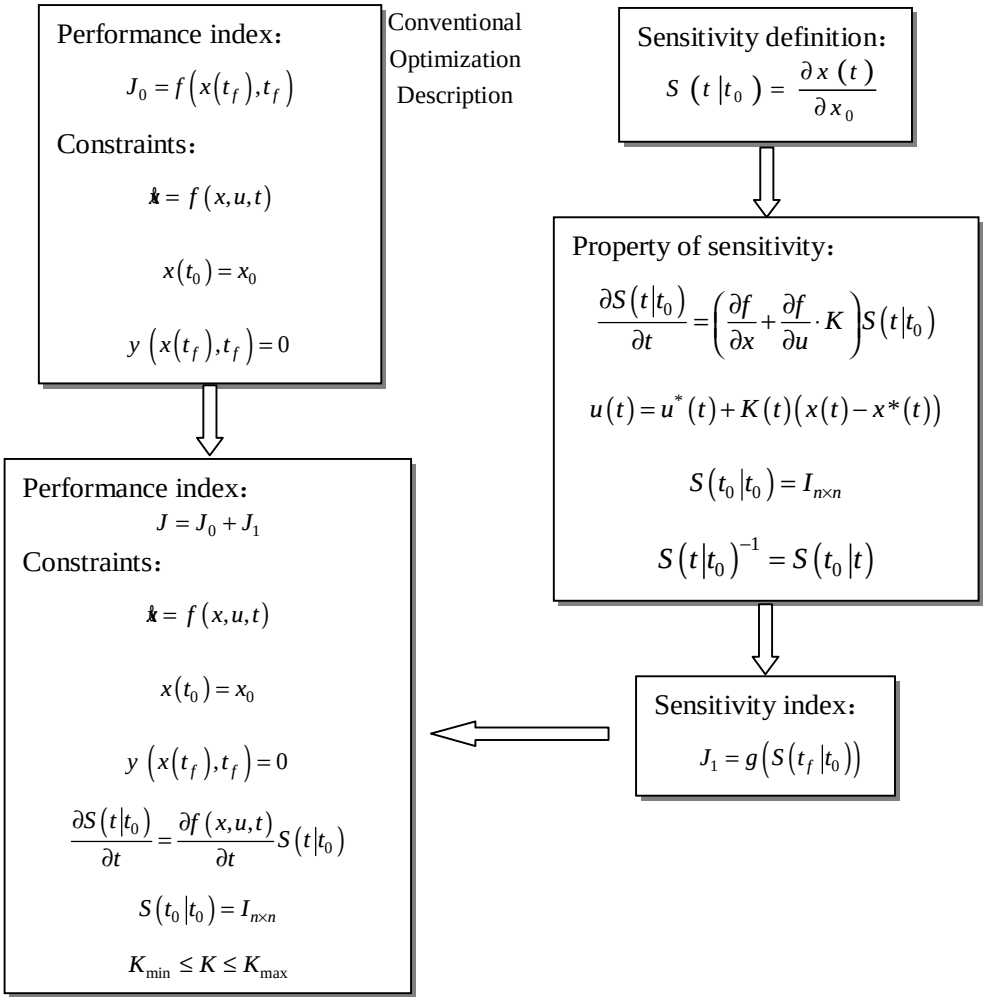


**Figure 2. Mathematical description of trajectory optimization problem considering sensitivity**

As shown in figure 2 and literature [8,10]. Firstly, the sensitivity matrix of system state variables with respect to uncertainties and perturbations along entry process is introduced, and the gain matrix of tracking guidance is contained into reference trajectory optimization process through dynamic equations with state sensitivity. Then, the performance index of state sensitivity is defined according to specific design requirements (e.g. terminal height, velocity and heading error can be combined and weighted to construct the performance index of state sensitivity), this performance index is a function of the state sensitivity. After that, a comprehensive performance index is constructed by using the weight factor method to combine the performance index of state sensitivity and original optimal performance index. Finally, this weighted optimization problem can be solved by direct or indirect methods. Here, we use the Gauss Pseudospectral Method (GPM) with Sequential Quadratic Programming (SQP) solver to process this compound optimization problem.

### 3.3 Optimal tracking guidance law

Based on the reference trajectory designed above, in this section, a close-loop tracking guidance law is designed using linear quadratic optimal strategy. The tracking guidance design is based on the trajectory error with respect to basic reference trajectory; the compensation control law is designed by Gauss pseudospectral method.

The tracking control problem is cast into a trajectory state regulation problem. The linearized dynamics of Eqs.(1)~(6) can be treated as the general form linear time varying system as following:

$$d\dot{\boldsymbol{x}}(t) = A(t)d\boldsymbol{x}(t) + B(t)d\boldsymbol{u}(t) \tag{20}$$

subject to the initial conditions $d\boldsymbol{x}(t_0) = d\boldsymbol{x}_0$ . Where $d\boldsymbol{x}(t) = [dr, dv, dg, dq, dl, dy]$ and $d\boldsymbol{u}(t)$ denote the differences between the actual and nominal values. The matrix $\boldsymbol{A}(t)$ and $\boldsymbol{B}(t)$ are obtained analytically from Eqs. (1)~(6). Their values depend on the state and control histories of the reference trajectory. The expressions of these matrixes are given in literature [11].

The problem is to determine the optimal control $d\boldsymbol{u}(t)$ and corresponding state vector $d\boldsymbol{x}(t)$ satisfying Eq. (20) while minimizing the quadratic performance function

$$J = \frac{1}{2}d\boldsymbol{x}^{\mathrm{T}}(t_f)Sd\boldsymbol{x}(t_f) + \frac{1}{2}\int_{t_0}^{t_f}\left[d\boldsymbol{x}^{\mathrm{T}}(t)Q(t)d\boldsymbol{x}(t) + d\boldsymbol{u}^{\mathrm{T}}(t)R(t)d\boldsymbol{u}(t)\right]dt \tag{21}$$

where, $S$ and $Q(t)$ are $n\times n$ symmetric positive semi-definite matrixes, $R(t)$ is $m\times m$ symmetric positive definite matrix. In eq. (21), terminal value item $\frac{1}{2}d\boldsymbol{x}^{\mathrm{T}}(t_f)Sd\boldsymbol{x}(t_f)$ reflects the requirement of terminal tracking error, integral item $\frac{1}{2}\int_{t_0}^{t_f} d\boldsymbol{u}^{\mathrm{T}}(t)Q(t)d\boldsymbol{u}(t)dt$ denotes the control cost, integral item $\frac{1}{2}\int_{t_0}^{t_f} d\boldsymbol{x}^{\mathrm{T}}(t)Q(t)d\boldsymbol{x}(t)dt$ reflects the requirement of dynamic tracking error.

Gauss pseudospectral method is utilized to process this problem and obtain the optimal compensation control $du$ which could suppress the unpredictable disturbance. The final real nominal command is consist of the basic reference command $u^*$ output by the trajectory optimization module and the optimal compensation control $du$, just as the follows.

$$u = u^* + du \tag{22}$$

## 4. Simulation Case

A preliminary simulation case is given to test the strategy mentioned above. The simulation parameters are set as follows. The initial constraints of the entry vehicle are $[r_0, v_0, g_0, s_0] = [3522000, 6000, -0.2, 0]$ ; its terminal constraints are $v(t_f) \le 350\text{m/s}$ and $s(t_f) = 935\text{km}$ ; peak overload is $n_{\max} = 8$ ; peak aerodynamic press is $q = 10000\text{kg/m}\cdot\text{s}^{-2}$ ; terminal aerodynamic press is $q_f \le 750\text{kg/m}\cdot\text{s}^{-2}$; peak heating rate is $\overline{q}_{f\max} = 70\text{kw/m}^2$; control constraints are $11.5\deg \le s \le 168.5\deg$ , $-20\deg/s \le \dot{s} \le 20\deg/s$ , $-5\deg/\text{s}^2 \le \ddot{s} \le 5\deg/\text{s}^2$ . Weight coefficients of sensitivity function are $c_1 = 1, c_2 = 1, c_3 = 0, c_4 = 0.01$ ; feedback gain is $\mathbf{k} = -[0.01 \quad 0.005 \quad 50 \quad 0.001]$. The uncertain parameters are set as shown in table 1.

Table 1. Uncertain parameters in simulation

| Item | Height | Velocity | Range | Atmospheric density | Ballistic coefficient | Lift-drag ratio |
|---|---|---|---|---|---|---|
| Initial value | 125km | 6000m/s | 0km | — | — | — |
| Error ( $3s$ ) | ±0.5 km | ±5 m/s | ±0.5 km | ±10% | ±5% | ±5% |

The simulation results is shown as follows.

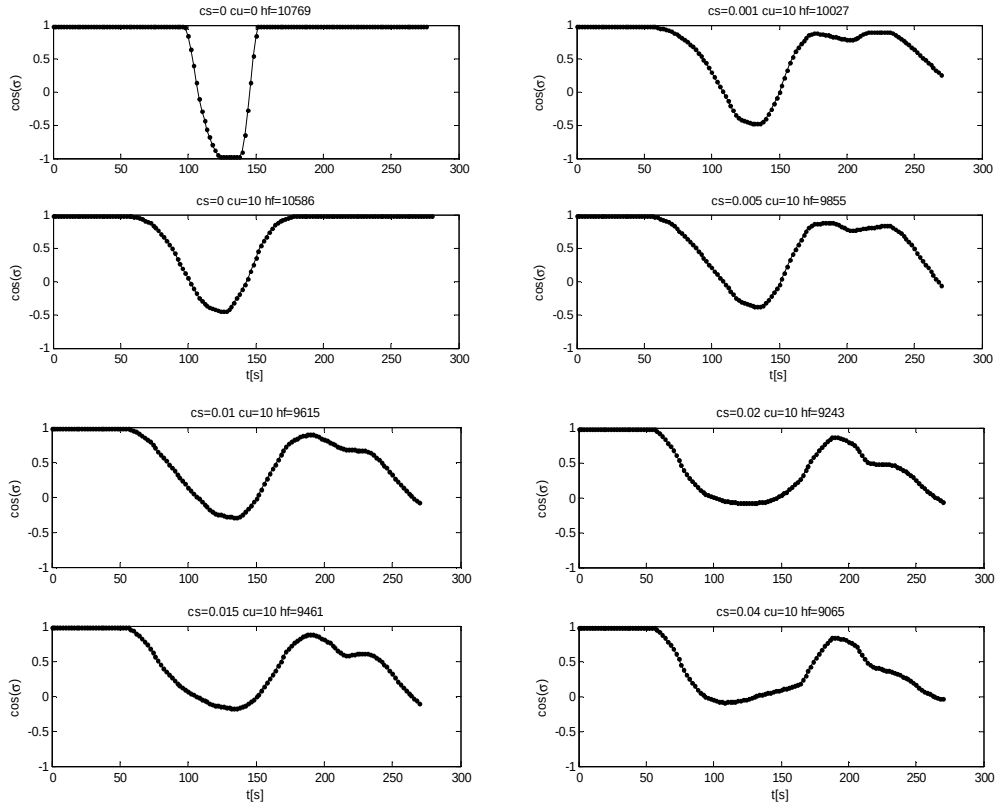


**Figure 3. Optimal command profile for Mars entry under different cases**

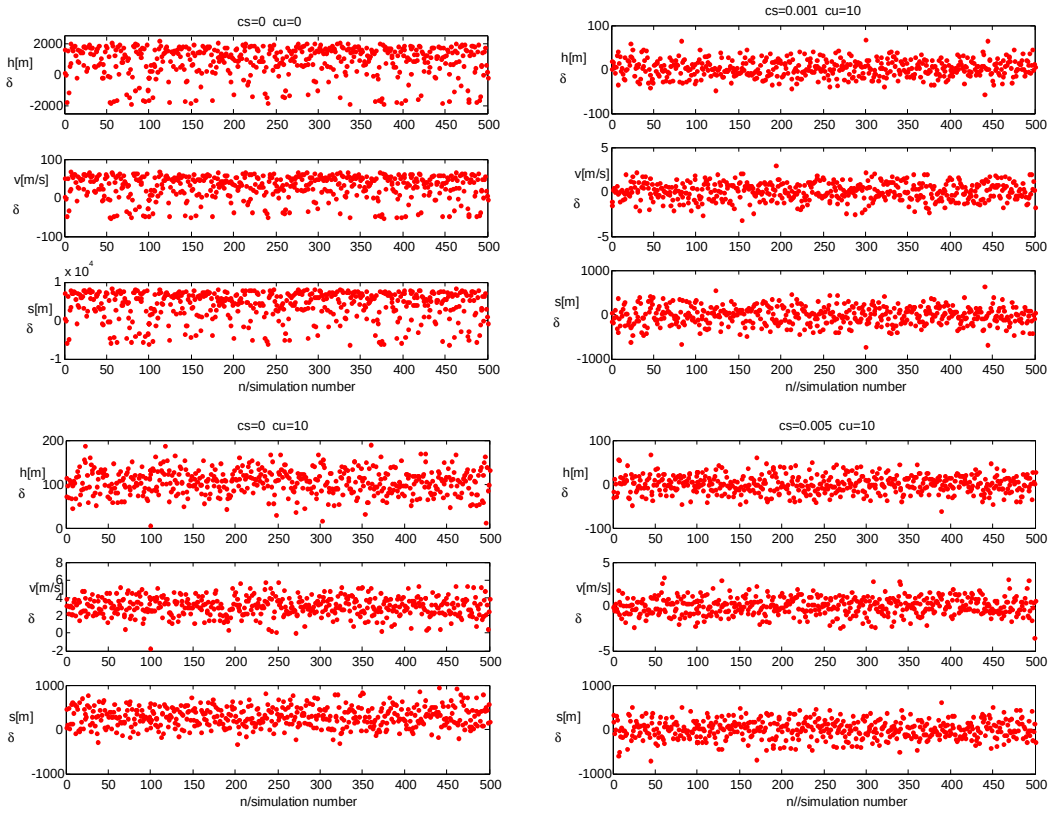


**Figure 4. Terminal state error analysis**

Figure 1 is the optimal control curve obtained by different weighted coefficient. We can found that: (1) most of optimal control profile is on the boundary of control constraint when $c_s = 0$ (performance function doesn't contain sensitivity), so the reference trajectory may be tracked hard in case some disturbance occur; (2) the control profile changes to more smoothness and less saturation when $c_u = 10$ (control efficiency is considered); (3) with the increasing of the $c_s$, optimal control profile is away from its constraint boundary so that the anti-disturbance performance is gradually enhanced but at the cost of lower terminal height.

For the real control profile obtained by using linear feedback control law to track the optimal trajectory, the larger $c_s$ is, the less saturation control would occur. Figure 2 shows the state error distribution on different value of $c_s$. From the figure 2, we can found that the terminal height, velocity, and range error are respectively about 2000m, 100m, 10km, when only terminal height is considered; and the error would be reduced when the fuel consumption is considered; and also the error would be further reduced when tracking performance is added to be considered. These results show that the method is effective.

## 5. Conclusions

To improve the accuracy and robustness of reference tracking guidance for Mars atmospheric entry, in this paper, we proposed a reference trajectory and optimal guidance integrated design strategy, which takes both the tracking efficiency of control system and the uncertainties during Mars atmospheric entry into account. Preliminary simulation test shows that this idea is feasible

and effective. It needs to be further and completely analyze, assess, and improve in our future work.

**Acknowledgements**

The work described in this paper was supported by the National Natural Science Foundation of China (Grant No. 61273051), Innovation Funded Project of Shanghai Aerospace Science and Technology (Grant No. SAST2015036), and Fundamental Research Funds for the Central Universities (Grant No. NS2014094). The authors fully appreciate their financial supports.

**References**

[1] Li, S., Jiang, X. Q., "Review and prospect of guidance and control technologies for Mars entry," Progress in Aerospace Sciences, Vol. 69, pp. 40-57, 2014.

[2] Jiang, X. Q., Wang, Y. K., Li, S., "Next-generation Mars EDL GNC: challenges and solutions," Proceedings of IEEE Chinese Guidance, Navigation and Control Conference, Yantai, China, 2014.

[3] Jiang, X. Q., Li, S., Liu, Y. F., "Innovative Mars EDL GNC technologies for future China Mars exploration," Proceedings of the 64th International Astronautical Congress, Beijing, China, 2013.

[4] Wolf, A. A., Casoliva, J., Manrique, J. B., et al, "Improving the landing precision of an MSL-class vehicle," Proceedings of IEEE Aerospace Conference, 2012

[5] Wolf, A. A., Acikmese, B., Cheng, Y., et al., "Toward improved landing precision on Mars," Proceedings of IEEE Aerospace Conference, 2011.

[6] Eduardo, G., Richard, G. W., Jeremy, D. S., et al., "Mars science laboratory entry guidance improvements study for the Mars 2018 mission," Proceedings of IEEE Aerospace Conference, 2012.

[7] Divya, V. S., Benjamin, R. G. E., Lethakumari, R., "Development of guidance algorithm for Mars entry," Proceedings of the 10th National Conference on Technological Trends (NCTT09'), 2009.

[8] Li, S. and Peng, Y. M. "Mars entry trajectory optimization using DOC and DCNLP." Advances in Space Research, Vol. 47, No. 3, pp. 440-452, 2011.

[9] Li, S., Jiang, X. Q. "RBF Neural Network based Second-order Sliding Mode Guidance for Mars Entry under Uncertainties." Aerospace Science and Technology, Vol. 43, pp. 226-235, 2015.

[10] Shen. H., Seywald, H., Powell, R. W. "Desensitizing the pin-point landing trajectory on Mars." Proceedings of AIAA/AAS Astrodynamics Specialist Conference, AIAA-2008-6943, 2008.

[11] Tian, B. and Zong, Q. "Optimal guidance for reentry vehicles based on indirect Legendre pseudospectral method." Acta Astronautica, Vol. 68, No. 7, pp.1176-1184, 2011.